

Peculiarities of oxide nanoparticle formation during metal droplet combustion

V.V. Karasev¹, A.A. Onischuk¹, S. A. Khromova¹, O. G. Glotov¹, V.E. Zarko¹,
E. A. Pilyugina¹, C.-J. Tsai², P. K. Hopke³

¹Institute of Chemical Kinetics and Combustion, RAS, Novosibirsk, Russia

²Institute of Environmental Eng., National Chiao Tung University, Hsinchu, Taiwan

³Clarkson University, 13699-5708, Potsdam, NY, USA

Abstract

Formation of metal oxide nanoparticles was studied during combustion of Al / Ti droplets moving in the air at the velocity of 10 - 300 m/s. A high energetic mixture was used composed by oxidizer, binder and metal particles (of size being varied between 4 and 350 μm) to ignite and eject the particles to the air as liquid burning droplets. Metal oxide nanoparticles were analyzed by a Transmission Electron Microscope. $\text{Al}_2\text{O}_3/\text{TiO}_2$ fractal aggregates were formed by the combustion of metal droplets with the size of 0.1 - 10 μm which consist of primary particles with the diameter of 5 - 50 nm. It was observed that in the case of Al droplet combustion oxide nanoparticles are formed in the reaction zone detached from the droplet surface. Both the ratio r/R_{reac} (between the droplet radius and the radius of the reaction zone) and the radius of primary particles in Al_2O_3 aggregates are functions of the droplet radius r . In the case of titanium the combustion zone was attached to the droplet surface; there was no dependency between the primary particle size and radius of the maternal Ti droplets. Very long aggregates of both Al_2O_3 and TiO_2 of length from a few tens to a few hundreds microns were observed which were attributed to the gelation process in the smoke tail.

The experimental data are reasonably described in terms of an analytical model considering diffusion of titanium oxide vapor (or Al and O_2), titanium oxide crystalline shell formation, TiO_2 droplet burst due to the nitrogen release followed by the inner droplet pressure increase. The model predicted that the titanium oxide nucleation occurs at the distance of about 10 μm from the burning surface at the critical supersaturation $S_{\text{crit}} \approx 3.5$. Then the nanoparticles are driven outwards by the thermophoresis.

1. Introduction

The investigations of single metal droplets combustion are inspired by both fundamental interest [1, 2] and possible applications [3]. In particular the combustion of metal powder can be an effective way of synthesis of semiconductor and ceramic oxide nanoparticles [3]. Metal powders are of interest as ingredients for high energetic formulations. Aluminum powders are added to propellants and explosives to boost their combustion enthalpy [2, 4, 5]. It has been recognized also that other metals like titanium, beryllium, zirconium can be useful as energetic additives in propellants, explosives and incendiaries [6]. In respect to these applications a single metal particle burning in air at 1 atm was selected by many researches (see, for example, [1, 7, 8]) as a simple model for theoretical and experimental study. Metal oxide nanoparticles are a product of maternal metal particle combustion. However the mechanism of nanoparticles formation is not understood completely yet, partially, due to the lack of experimental data

The objective of this study is to investigate the mechanism of TiO_2 and Al_2O_3 nanoparticle formation during combustion of Ti and Al droplets in air at atmospheric pressure. The main questions under consideration were metal oxide nanoparticle size, morphology, mobility as well as stages of combustion of maternal droplets.

2. Experimental

Metal oxide nanoparticles were formed by combustion of Al or Ti droplets moving in the air at atmospheric pressure. Two types of experiments were carried out. In the first case a single particles of diameter 100 - 350 μm were charged into a quartz capillary together with an igniting composition. The capillary inner diameter was 0.2 cm. The igniting composition consisted of oxidizer and binder and served to ignite the particles and eject them one after another to the ambient air with the velocity of 100 - 300 cm/s. The moving burning droplet was recorded by a high speed video camera. The droplet collided at a small angle with a special glass support covered by a formval film (trade mark - "Formvar") so that the metal oxide nanoparticles were freezed at the early stage of growth. As a result the nanoparticle deposit was formed at the surface. The deposit distribution was analyzed by an optical microscope. Finally the Formvar film with deposit was detached from the surface put to the copper electron microscopy grid and analyzed using an Transmission Electron Microscope (TEM). The main advantage of this technique was that the quenched deposited nanoparticles gave an insight to the earliest stages (10^{-4} sec) of particle growth. The time of droplet flight was

varied by the change of distance between the capillary and the surface and was in the range between 50 - 100 ms.

The second type of experiments included the metal oxide nanoparticle formation by combustion of pyrotechnic mixture in a reaction camera. This experimental approach was described in details in refs [9].

3. Experimental results

Pyrotechnic mixture combustion results in generation of Al_2O_3 / TiO_2 nanoparticles which are formed as aerosol aggregates of size 0.1 - 10 μm composed by small primary nanoparticles of diameter between 5 - 50 nm [9]. Typical example of aggregates is shown in Fig. 1. The X-ray diffraction analysis showed that titania nanoparticles consist of anatase (40%) and rutile (60%) phases. The alumina nanoparticles were composed by a mixture of α and γ phases of Al_2O_3 .

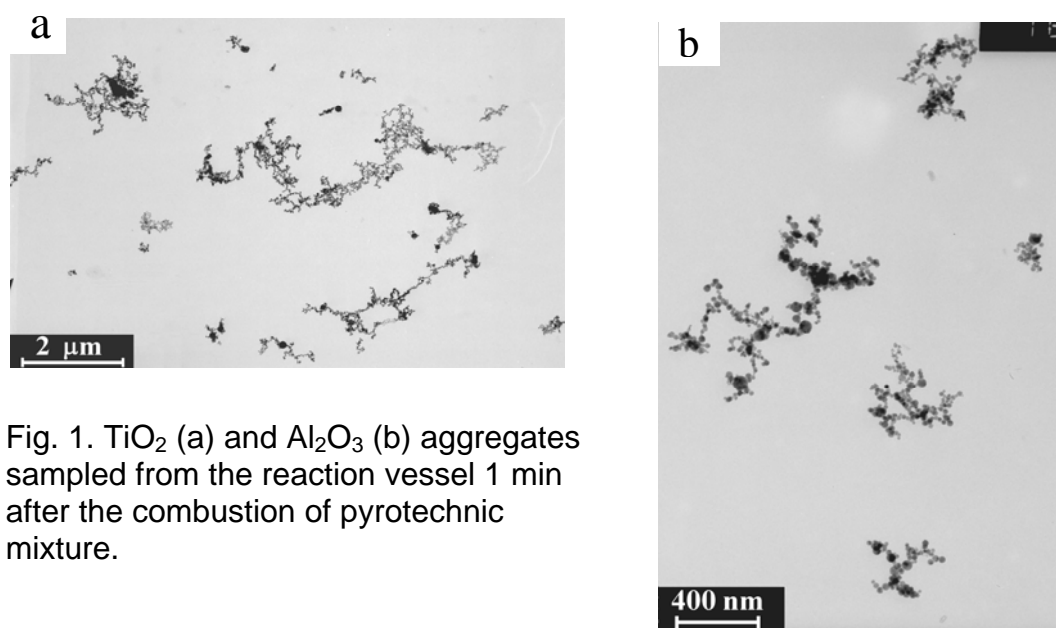


Fig. 1. TiO_2 (a) and Al_2O_3 (b) aggregates sampled from the reaction vessel 1 min after the combustion of pyrotechnic mixture.

We found that in the case of Al_2O_3 the primary particle size distribution is a function of diameter of the maternal droplet (Fig. 2). In these experiments we used an igniting composition filled by Al particles with the mean diameter of 4, 110 and 340 μm and polydisperse powder with the mean arithmetic diameter of 18 μm . The size distribution for monodisperse and polydisperse powders was good described by the lognormal function with the standard geometric deviation to be 1.1 and 2.0, respectively. The dependency of the mean primary particle diameter on the original Al powder diameter is given in Fig. 3. On the contrary, in the case of TiO_2 aggregates we did not find any correlation between the original powder size and primary particle

size distribution. Fig. 4 shows size distributions for primary particles formed by combustion of single 330 μm droplets and pyrotechnic mixture containing Ti powder of diameter $< 20 \mu\text{m}$. In the first case the primary particle mean diameter was 22.4 nm, in the second case it was 22.7 nm.

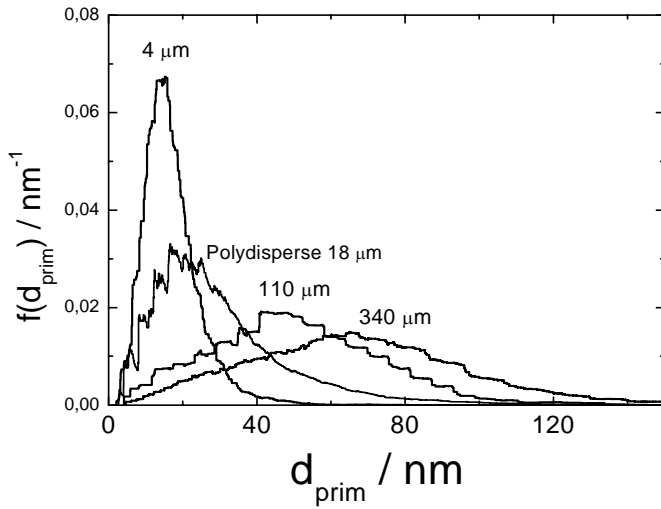


Fig. 2. Primary particle diameter distribution for Al_2O_3 aggregates formed by the combustion of pyrotechnic mixtures with monodisperse Al powder of diameter 4, 110 and 340 μm and polydisperse powder with the mean diameter of 18 μm (shown in the Figure).

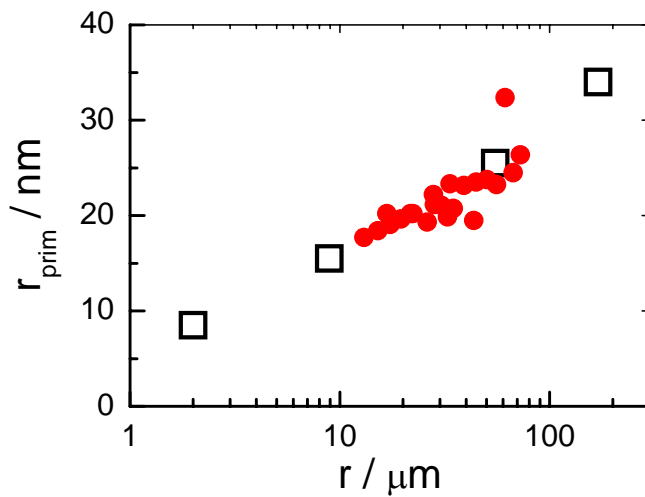


Fig. 3. Mean arithmetic diameter of primary particles vs. diameter of original Al particle in the pyrotechnic mixture as measured experimentally (squares) and evaluated using a simple model (circles, see sec4.1 and data from fig 9)

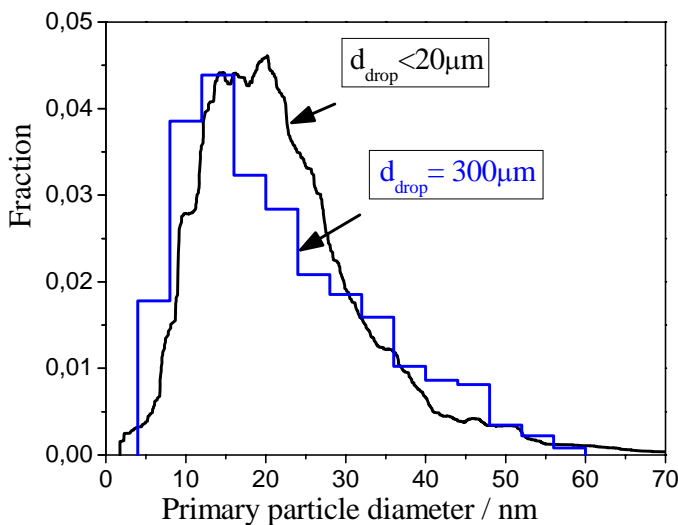


Fig.4. Frequency distribution of diameters of primary particles in TiO_2 aggregates formed by combustion of single 330 μm droplets and pyrotechnic mixture containing Ti powder of diameter $< 20 \mu\text{m}$.

The combustion scenario for single Al and Ti droplets was quite different. At the final stage of Al droplet combustion the flame died out gradually as a rule, during the period 1 - 3 ms. In the case of Ti all the droplets have finished the combustion by the burst. In more detail the stages of the burst are shown in Fig. 5. Initial frame ($\tau = 0$ ms) demonstrates the movement of the burning droplet (marked by symbol 1). The bright stroke in the frame is the trajectory covered by the droplet during the time 0.9 ms. At the next frame this droplet burst out ($\tau = 1$ ms).

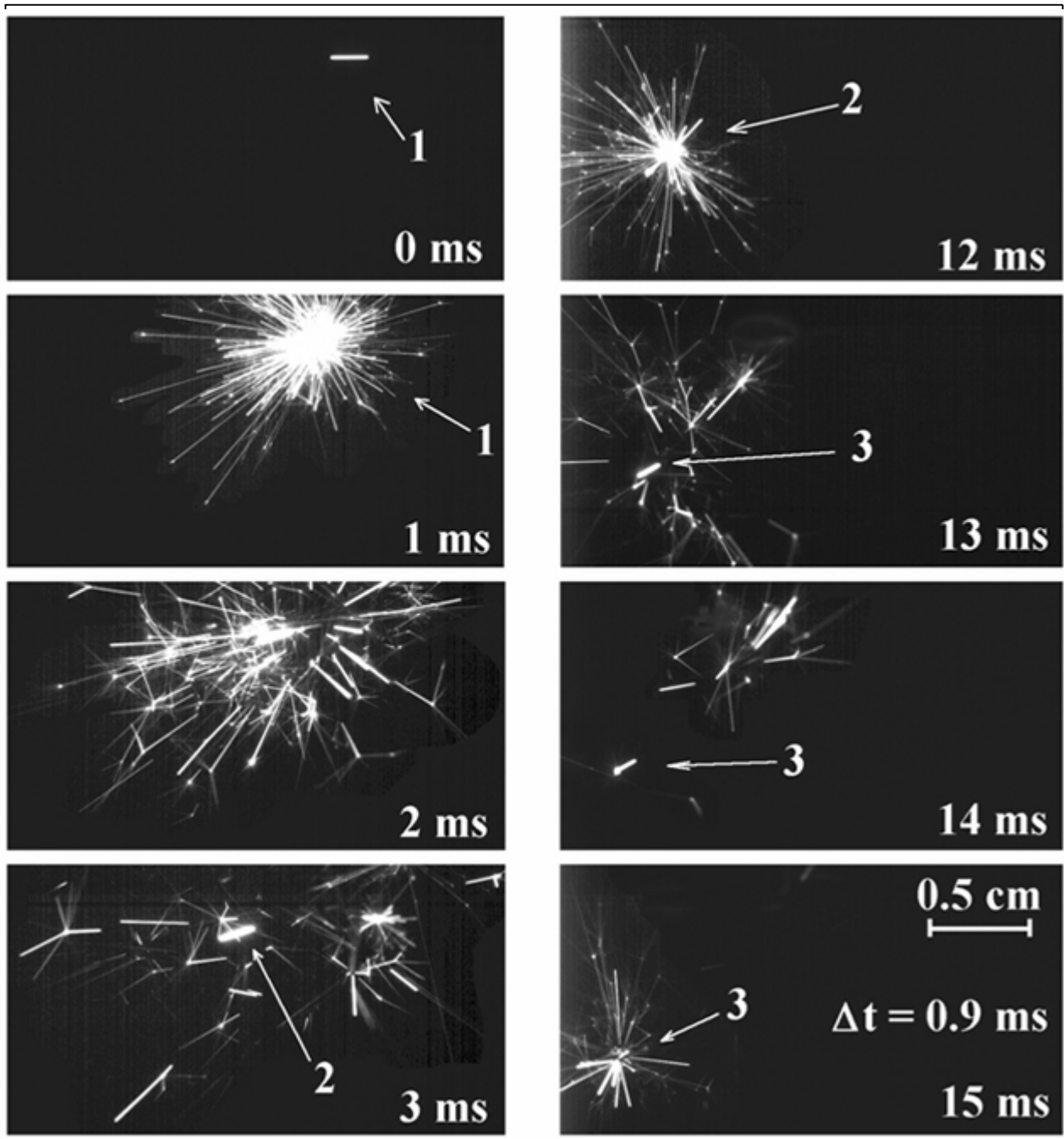


Fig. 5. Consequence of frames illustrating the burst at the last stage of combustion of Ti droplet. The droplet initial diameter is 200 μm ; frame duration 0.9 ms. The initial time for each frame is shown in the figure.

One can see the most of fragments are exploding again at during the time $\tau = 1 - 3$ ms. In some cases there is a consequence of bursts. Thus, the fragment 3 exploding in the last frame ($\tau = 15$ ms) is a product of the burst of the fragment 2 ($\tau = 12$ ms). The magnified image of the burning *Al* droplet is shown in Fig. 6. One can see clear the detached reaction zone (seen as a halo) where the aluminum oxide nanoparticles are formed in the reaction between *Al* vapor and atmospheric oxygen.

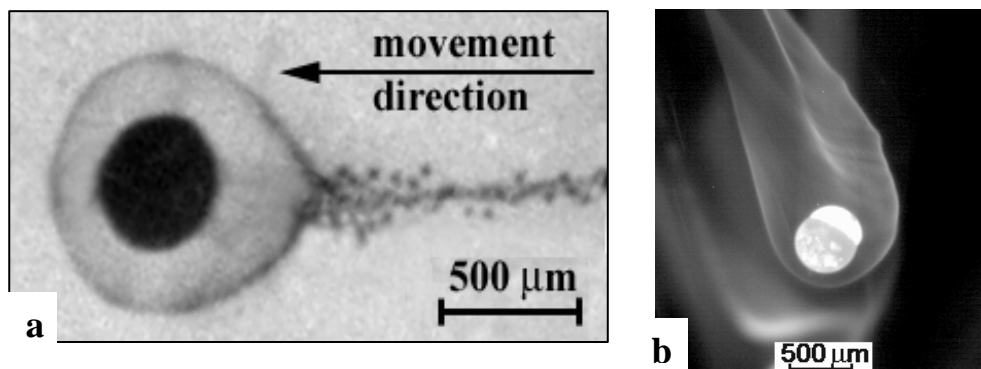


Fig. 6. Burning *Al* droplet; a) shadow image in the blue back light, b) self irradiance image.

In some cases very large aggregates with the diameter from a few tens to a few hundred microns were observed in the "smoke tail" (Fig. 6a, 7a, 8a).

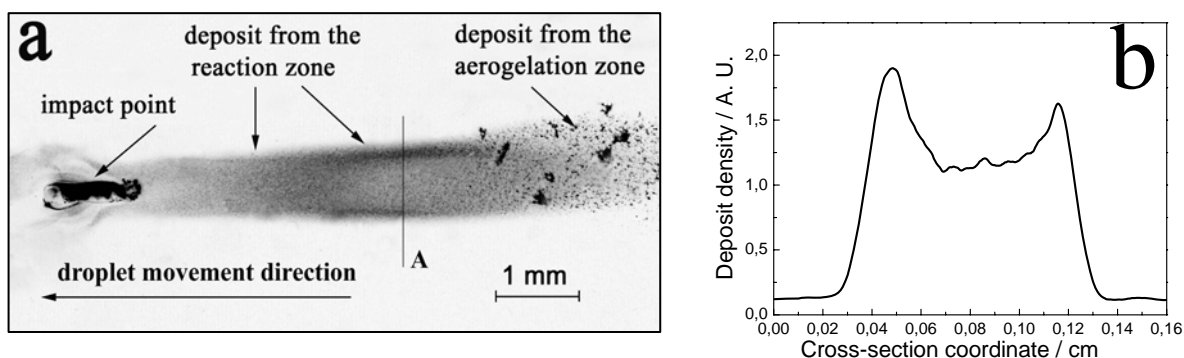


Fig. 7. a) Optical microscope image of a deposit formed at the glass surface due to the impact of burning *Al* droplet at small angle; b) density profile of the deposit at location A. The diameter of maternal droplet is 300 μm .

One can see also an oxide cap on the surface of *Al* droplet (Fig. 6b). We found that the radius of the reaction zone is a function of the drop radius. The ratio between the radius of halo and that of the droplet is presented in Fig. 9 for the droplets moving with the velocity of about 1000 cm/s. Fig. 10 shows the oxide smoke tail formed during the combustion of *Ti* droplet. One can see that there is no detached reaction zone (as in contrast to the case of *Al*); the titanium oxide nanoparticles are formed just near the droplet surface.

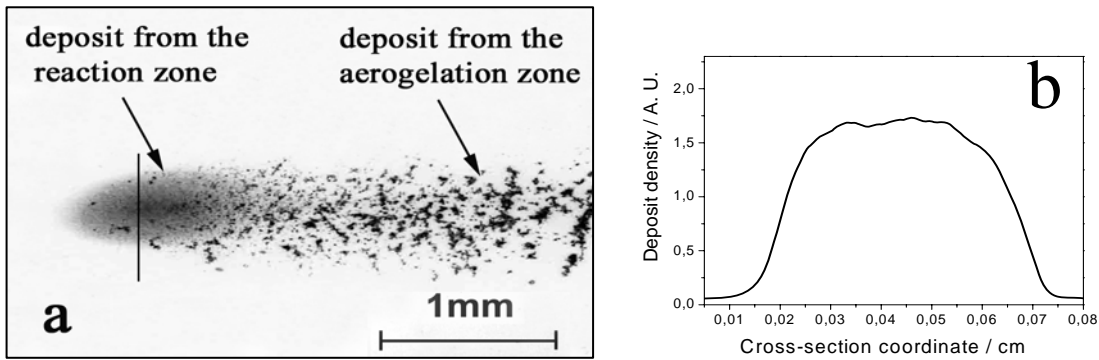


Fig. 8. a) Optical microscope image of a deposit formed at the surface due to the impact of burning Ti droplet at small angle; b) density profile of the Ti deposit from the reaction zone. The diameter of maternal droplet is 330 μm .

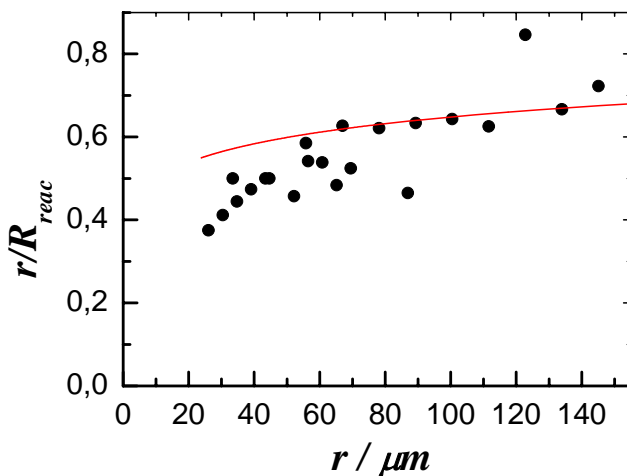


Fig. 9. Ratio between the radius of halo and that of the droplet vs. radius of Al droplet (symbols). The air counter flow velocity is about 1000 cm/s.

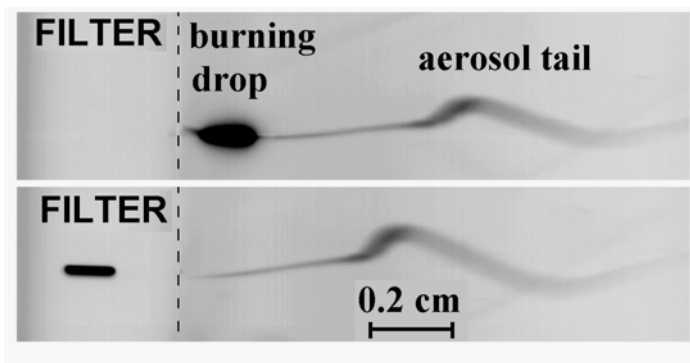


Fig. 10. Two consecutive frames (negatives) of the burning Ti droplet in the 90° scattered light. The initial droplet diameter is 200 μm . Frame frequency is 1 KHz, frame duration is 0.9 ms. The left side of the frame is filtered to avoid the droplet over irradiance (to measure the droplet diameter).

To make an insight to the initial stages of oxide nanoparticle formation the combustion process was frozen by the collision of burning droplet with a glass surface at a small angle. Figs. 7a and 8a show optical microscope images of deposits formed by deposition of Al and Ti droplets and density profiles for these images. The deposit density profiles for Al_2O_3 and TiO_2 (Figs. 7b and 8b) are quite different. In the case of Al_2O_3 two maximums are clearly seen corresponding to nanoparticles from the detached reaction zone (see also Fig. 6); in the case of TiO_2 there is a bell-shaped density distribution in the central part of the deposit indicating to the fact that the reaction with

oxygen is attached to the droplet surface. TEM images for TiO₂ deposit are shown in Fig. 11. One can see that near the droplet surface there are single particles and relatively small aggregates. On the other hand, there are very long chain-like aerosol aggregates in the smoke tail [13].

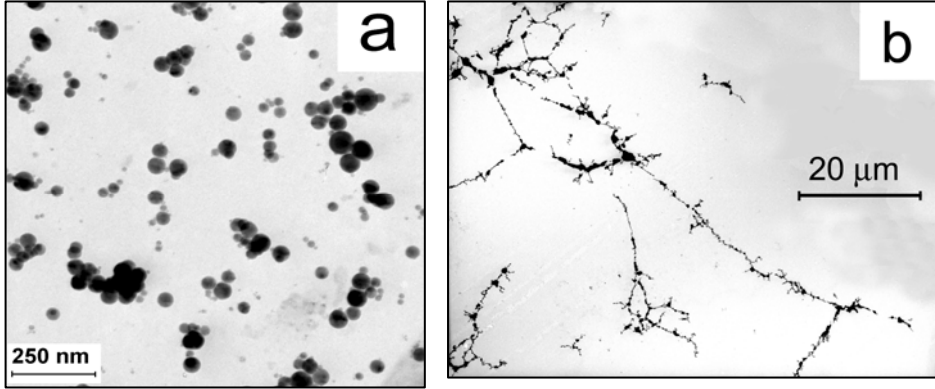


Fig. 19. TEM images of TiO₂ nanoparticles deposited on the substrate by combustion of single Ti droplet: a - from the reaction zone, b - from the aerogelation zone [13].

4. Discussion

4.1. Details of Al droplet combustion

To explain the experimentally determined dependence of Al₂O₃ nanoparticle size on the diameter of maternal droplet we elaborated a simple model. In this model the position of the reaction zone with respect to the droplet surface was determined solving the diffusion equations for oxygen and Al vapor coupled with the heat conductivity equations. It was taking into account that the ratio

$$\frac{D_{Al}}{D_{O_2}} = \sqrt{\frac{\mu_{O_2-N_2} \sigma_{O_2-N_2}}{\mu_{Al-N_2} \sigma_{Al-N_2}}} \approx 1.34 \quad [12],$$

where D_{Al} and D_{O_2} are diffusion coefficient for Al atoms and O₂ molecules, $\mu_{O_2-N_2} = \frac{m_{O_2}m_{N_2}}{m_{O_2} + m_{N_2}}$; $\mu_{Al-N_2} = \frac{m_{Al}m_{N_2}}{m_{Al} + m_{N_2}}$; m_{Al} , m_{O_2} , m_{N_2} are

mass of Al, O₂ and N₂, respectively, $\sigma_{O_2-N_2}$ and σ_{Al-N_2} are collision cross sections between O₂ and N₂ and Al and O₂, respectively. An equation was derived based on this model:

$$\frac{r}{R_{reac}} \approx \left(0.5(1-0.5\alpha) + \sqrt{\alpha^2 + 10\alpha + 1}\right)^{-1}, \quad (1)$$

where R_{reac} is radius of reaction zone, r is maternal radius, $\alpha = 0.5\sqrt{D_{O_2}\tau}$, τ is

characteristic time $\tau = \frac{R_{reac}}{V}$, V is air counter flow velocity in the reaction zone. The

ratio $\frac{r}{R_{\text{reac}}}$ as calculated via Eq. (1) is shown in Fig. 9 as a function of droplet radius.

One can see a reasonable agreement between the experimental data and the calculation results. The model predicts the radius of primary particles as a function of the maternal droplet radius (Fig. 3) which is in a reasonable agreement with the experimental values.

4.2. Details of Ti droplet combustion

After the ignition the temperature of liquid *Ti* droplet is rapidly increasing due to the oxygen diffusion from the ambient atmosphere to the surface followed by the energy release [8]. Since both oxygen and nitrogen diffuse to the droplet from the air the Ti - O - N solution is formed. As shown in [8] the concentration of nitrogen in the burning droplet is about 10 at. % which is not enough to form the solid phase TiN. The temperature of the burning droplet is increasing during the first 150 ms up to about 2700 K, then it falls down to about 2200 K and the process terminates by the explosion [8] (see also Fig. 5). The temperature decrease at the time > 150 ms is probably related to the decrease of the rate of heat release because of the oxygen radial profile in the droplet becoming less steep (i.e. oxygen diffusion becoming more slow). Finally, the temperature reaches the solidification point. The average oxygen concentration is about 40 at. % at that moment [8]; at the surface the concentration is higher. The higher oxygen concentration the higher is the phase transition temperature. In the case of Ti - O system the phase transition temperature would be about 2100 K. Two solid phases TiO + Ti₂O₃ are forming. The solid phase formation starts probably on the front side of the moving droplet which should be colder due to the counter flow of the air. The formation of the solid shell results in the nitrogen release to the inner part of the particle. When the solid shell is formed around the liquid droplet the inner droplet pressure starts to increase due to the nitrogen release. The droplet burst occurs because the solid shell strength is less than the inner pressure. Thus, the stretching breaking force limit for the solid shell can be estimated as:

$$F_{\text{lim}} = 4\pi\sigma[R^2 - (R - \delta)^2] \quad (2)$$

where $\sigma = 40$ MPa is breaking force limit per unit surface, R is outer radius of the solid shell, δ is the solid shell thickness (i.e. the difference between the outer radius of the shell and the radius of liquid core). Analyzing the video microscopy images for bursting droplets we found that the average velocity for the debris generated by the

droplet with diameter of 100 μm is $v_{av} \approx 360$ cm/s. Thus, the kinetic energy for these fragments is in average $E_{kin} = \frac{mV^2}{2} \approx 0.14$ erg, where m is mass of droplet. Each droplet bursts in average into about one hundred fragments. Thus, the increase of the surface energy E_{surf} due to the additional surface from the newly formed fragments can be estimated using the surface tension for titania $\gamma \approx 270$ dyne/cm [11] as $E_{surf} = 0.31$ erg. Thus, the energy consumed for liquid dispergation is $E_{tot} = E_{kin} + E_{surf} = 0.45$ erg. One should understand that this energy is a part of the over pressure work, the other part is the gas expansion work produced during the droplet explosion. We can evaluate the lowest limit for the over pressure assuming that the energy E_{tot} is equal to the over pressure work W . Using the Van't-Hoff's law for the over pressure from the gas dissolved one have for the case of solid shell being thin with respect to the droplet radius r :

$$W = \xi RT \ln\left(\frac{P_{in}}{P_0}\right) \approx \xi RT \ln\left(\frac{\xi RT}{\frac{4}{3}\pi R_{drop}^3 P_0}\right) \quad (3)$$

where P_{in} and P_0 are inner pressure and atmospheric pressure, respectively, ξ is number of moles. Using the values $r = 5 \times 10^{-3}$ cm, $W = 0.45$ erg, $T = 2100$ K we get the solution of Eq.(3) $\xi = 5.1 \times 10^{-12}$ which corresponds to the inner pressure $P_{in} = 1.7 \times 10^5$ Pa. The balance between the inner pressure and the stretching breaking force limit for the solid shell will result in the breaking over pressure:

$$P_{in} = \left[\left(1 - \frac{\delta}{R_{drop}}\right)^{-2} - 1 \right] \sigma \quad (4)$$

where δ is solid shell thickness. Thus, one gets from Eq. (4) $\delta \approx 5 \times 10^{-6}$ cm. Using this value of δ and the magnitude for inner pressure we have the nitrogen concentration in the surface layers of the droplet juts before the burst $C_N \approx 8$ at. %. This value of C_N can be considered as the lowest limit for nitrogen concentration which is in a qualitative agreement with the experimental measurements of Molodetsky et al. [8] demonstrating the nitrogen concentration to be about 10 at.% for the droplet with the diameter of 240 μm .

Conclusions

The experimental results demonstrate that combustion of Al and Ti droplets results in formation of TiO_2 and Al_2O_3 aerosol aggregates with the size of 0.1 - 10 μm which consist of primary particles with the diameter of 5 - 50 nm. It was found that both the ratio $\varphi = \frac{r}{R_{\text{reac}}}$ (between the droplet radius and the radius of the reaction zone) and the radius of primary particles in Al_2O_3 aggregates are functions of r . This dependences are reasonably explained by a simple diffusion model.

The combustion of Ti droplet was found to proceed via a consequence of bursts. A simple model was analysed assuming that the reason for bursts lies in the crystal shell formation followed by the nitrogen release and the droplet inner pressure increase as a consequence. Estimating the dispergation energy for the droplet as a sum of the debris kinetic energy and surface energy increase due to the newly formed surface we get the inner breaking pressure $P_{\text{inn}} = 1.7 \times 10^5$ Pa which corresponds to the concentration nitrogen dissolved in the liquid droplet to be about 8 at. %.

We evaluated the critical supersaturation $S_{\text{crit}} \approx 3.5$ for the titanium oxide vapor near the surface using a simple diffusion model. The estimations showed that the nucleation occurs at about 10 μm from the burning surface. Then the nanoparticles are driven outwards by the thermophoresis.

Very long aggregates of both Al_2O_3 and TiO_2 of length from a few tens to a few hundreds microns were observed which were attributed to the gelation process in the smoke tail.

ACKNOWLEDGMENTS

Financial support for this work was provided by INTAS foundation _Grant No. 03-53-5203_, Russian Foundation for Basic Research _RFBR_ _Project Nos. 04-03-33162, 04-03-33163, 05-03-90576-NSC_a, and 05-02-08290- OFI_a_, NSC_Taiwan_-RFBR No. 94WFA0600016 _Contract No. RP05E15., ISTC grant No 3305.

References

1. E. L. Dreizin. Experimental study of aluminum particle evolution in normal and micro-gravity. *Combustion and Flame*, 1999, Vol. 116, pp. 323-333.

2. Price E. W., Sigman R. K. Combustion of aluminized solid propellants. In: Solid Propellant Chemistry, Combustion, and Motor Interior Ballistics / Edited by V. Yang, T. B. Brill, Wu-Zhen Ren. Progress in Astronautics and Aeronautics, V. 185. Editor-in-Chief P.Zarchan. Publ. by AIAA Inc., Reston, VA, 2000. Ch. 2.18. pp. 663-687.
3. A. N. Zolotko, Ya. I. Vovchuk, N. I. Poletaev, A. V. Floriko, I. S. Altman Synthesis of nanooxides in two-phase laminar flames. *Combustion, explosion, and Shock Waves*, 1996, 32 (3), 24 - 33.
4. T. A. Brzustowski and I. Glassman, "Vapor-phase diffusion flames in magnesium and aluminum combustion. 1. Analytical study," in: H. G. Wolfhard, I. Glassman, and L. Green (eds.), *Heterogeneous Combustion*, Academic Press, New York (1964), pp. 75–115.
5. E. W. Price and R. K. Sigman, "Combustion of aluminized solid propellants," in: V. Yang, T. B. Brill, and Wu-Zhen Ren (eds.), *Progress in Astronautics and Aeronautics*, Vol. 185: Solid Propellant Chemistry, Combustion, and Motor Interior Ballistics, Ch. 2.18. AIAA Inc., Reston, VA (2000), pp. 663–687.
6. E. L. Dreizin, Phase changes in metal combustion, *Progress in Energy and Combustion Science* 2000, 26, 57 - 78.
7. P. Bucher, R. A. Yetter, F. L. Dryer, T. P. Parr, D. M. Hanson-Parr, E. P. Vicenzi. Flame structure measurement of single, isolated aluminum particles burning in air 26th Symp.(Int.) on Combustion. The Combustion Institute, 1996. pp. 1899 - 1908.
8. I. E. Molodetsky, E. P. Vicenzi, E. L. Dreizin, C. K. Law, Phases of Titanium Combustion in Air. *Combustion and Flame* 1998, 112, 522 - 532
9. V. V. Karasev, A. A. Onischuk, O. G. Glotov, A. M. Baklanov, A. G. Maryasov, V. E. Zarko, V. N. Panfilov, A.I. Levykin, K. K. Sabelfeld, Formation of charged aggregates of Al_2O_3 nanoparticles by combustion of aluminum droplets in air. *Combustion and Flame*, 2004, 138, 40 - 54.
10. S. K. Friedlander, *Smoke Dust and Haze*, Oxford University Press, New York/Oxford, 2000.
11. Physical magnitudes (reference-book) Eds. I. S. Grigoriev, E. Z. Meylikhov, Energoatomizdat, Moscow, 1991.
12. RC Reid, JM Prausnitz, and TK Sherwood, *The properties of gases and liquids*, McGrawHill, New York, 4th. edition, 1987.
13. C. M. Sorensen, W. B. Hageman, T. J. Rush, H. Huang, and C. Oh, Aerogelation in a Flame Soot Aerosol. *PHYS. REVIEW LETTERS* 80 , 1783 - 1785, 1998